Progress In Electromagnetics Research M, Vol. 85, 95–104, 2019

Design of a Four-Element MIMO Antenna with Low Mutual Coupling in a Small Size for Satellite Applications

Aziz Dkiouak[1, *], Alia Zakriti[1], Mohssine El Ouahabi[1], Naima A. Touhami[2], and Aicha Mchbal[2]

Abstract—In this paper, a compact planar mono-band multiple input multiple output (MIMO) antenna with four monopole elements is presented for X-band satellite applications (7.2–7.8 GHz). The MIMO antenna resonates at 7.5 GHz, with high isolation (more than 26 dB) between its ports. It consists of a four closely arranged symmetric monopole antennas with edge-to-edge distance of 7.2 mm (0.18λ). In the top face, different forms are loaded at the rectangular patch. A U-shaped slot defected ground structure (DGS) has embedded in the ground plane. The prototype of the proposed MIMO antenna is simulated, fabricated, and measured to examine the performance of this antenna in terms of S parameters, radiation patterns, envelope of correlation coefficient (ECC), and diversity gain (DG). As a result, the presented antenna has a high isolation ($S_{12} < -26$ dB) at 7.5 GHz with an impedance bandwidth of 430 MHz (7.28 GHz–7.71 GHz), which covers the X-band applications. The diversity gain is about 10, and the envelope correlation coefficient of antenna is less than 0.02 which means that the antenna has high performance at the resonance frequency.

1. INTRODUCTION

In future generation of wireless communication networks, high data transmission rate and low bit error probability have been common requirements. Most of the research in this area focuses on the deployment of new technologies to make wireless networks perform better and better. Multiple input multiple output (MIMO) antennas are considered as a great solution for improving transmission reliability by reducing the probability of error (diversity gain), increasing the transmission data rate (multiplexing gain), decreasing multiple fading, and increasing channel capacity [1]. The MIMO technology is regarded as a key of the 3G, 4G, and the future 5G wireless data communications. The critical point of MIMO system design is to increase the isolation between the antenna elements that affects wireless channels, the diversity performance, as well as channel capacity.

In MIMO systems, antennas are designed to ensure that the mutual coupling among their elements is lower than -12 dB [2].

Recently, there are many techniques that have been used in the literature to reduce the mutual coupling between antennas, and much effort has been devoted to minimizing the size of microstrip antennas such as using a dielectric substrate of high permittivity [3]. In [4–9], the mutual coupling between ports can be reduced by using defected ground structures (DGS) at the ground plane. In other words, the utilization of electromagnetic band gap (EBG) structure has the ability to enhance the isolation as well as increase the MIMO antenna performance [10–12]. The work in [13] presents a MIMO antenna with improved isolation using meta-material structure. In [14–16], several x-band MIMO antennas with different techniques were designed and fabricated.

Received 12 July 2019, Accepted 4 September 2019, Scheduled 20 September 2019

* Corresponding author: Aziz Dkiouak (dkiouakaziz@hotmail.fr).

[1] National School of Applied Sciences, Abdelmalek Essaadi University, Tetuan, Morocco. [2] Faculty of Sciences, Abdelmalek Essaadi University, Tetuan, Morocco.

Several studies and new techniques have designed a MIMO antenna with low mutual coupling, small size, and low envelope correlation coefficient. Sun and Wei [17] have analyzed and designed 4×4 MIMO-antenna systems in mobile phone for ISM (2.4 GHz) applications. A design approach for dual-element hybrid MIMO antenna arrangement for wideband applications is proposed in [18], and a Meta-Surface Antenna Array Decoupling (MAAD) Method for Mutual Coupling Reduction in a MIMO Antenna System is presented in [19] by introducing periodic split ring resonators (SRRs) on the metasurface.

In this paper, we design a miniaturized four-element MIMO antenna with high isolation for satellite communications. The mono-band MIMO antenna is developed by using different forms loaded at a rectangular patch in order to adapt the resonant frequency at 7.5 GHz and to increase the effective capacitance and inductance, which influences the input impedance and current flow of the antenna and thus, reducing its size. The position of the etched U-slot in the ground plane is optimized to improve the isolation between antenna elements. The overall dimension of this antenna is $40 \times 40 \times 1.6\,\text{mm}^3$ ($0.47\lambda_g \times 0.47\lambda_g \times 0.08\lambda_g$, where λ_g = guided wavelength at the lowest frequency of operation). Meanwhile, the proposed MIMO antenna is compact in size, simple in structure, and easy in fabrication.

2. ANTENNA & DESIGN

2.1. Single Element Antenna

The design evolution of a single element compact microstrip antenna of the quad-element is illustrated in Figure 1(a), and the antennas' design procedure is simulated, and the corresponding reflection coefficient S_{11} curves are plotted in Figure 1(b). In this design, an FR4 substrate is used due to its low cost and easy fabrication with dimensions $20 \times 20 \times 1.6\,\text{mm}^3$. The relative permittivity and loss tangent of FR4 are 4.4 and 0.02, respectively. The antenna element is fed by a $50\,\Omega$ microstrip line for the excitation. The initial design approach is started with a rectangular monopole antenna at the top face and with an etched U-slot in the ground plane as shown in Figure 1 (Ant.0). As can be seen in Figure 1(b), a resonant frequency of 7.2 GHz is created. In Figure 1 (Ant.1), the resonance frequency is shifted to 7.4 GHz with slight enhancement in the impedance matching of the rectangular patch antenna by a rectangular shaped slot loaded on the surface of the patch. In Figure 1 (Ant.2), the corresponding result shows an improvement in the adaptation around 7.5 GHz by making modifications in the microstrip and the U-shaped slot together. The final design of the proposed antenna can be obtained in Figure 1 (Ant.3), with detailed dimensions as described in Table 1. The impedance matching of this antenna is much better than others, which is improved to 42 dB at the X-band satellite communication (7.2–7.8 GHz) as shown in Figure 1(b).

An antenna optimization is designed by using Computer Simulation Technology (CST) Microwave Studio Software, and after regressive optimization, the optimized dimensions of the antenna single element are illustrated in Table 1, as shown in Figure 2 with the overall volume of $20 \times 20 \times 1.6\,\text{mm}^3$.

Table 1. Dimensions of the proposed MIMO antenna.

Parameters	Values (mm)	Parameters	Values (mm)
L	40	W	40
$L1$	16.5	Wf	3.14
$L2$	8	Ws	10.5
$D2$	6.5	U	12.5
Lu	23.5	V	6.6
Ls	6.2	b	2
s	3	$D1$	7.2
a	1	Du	10.5

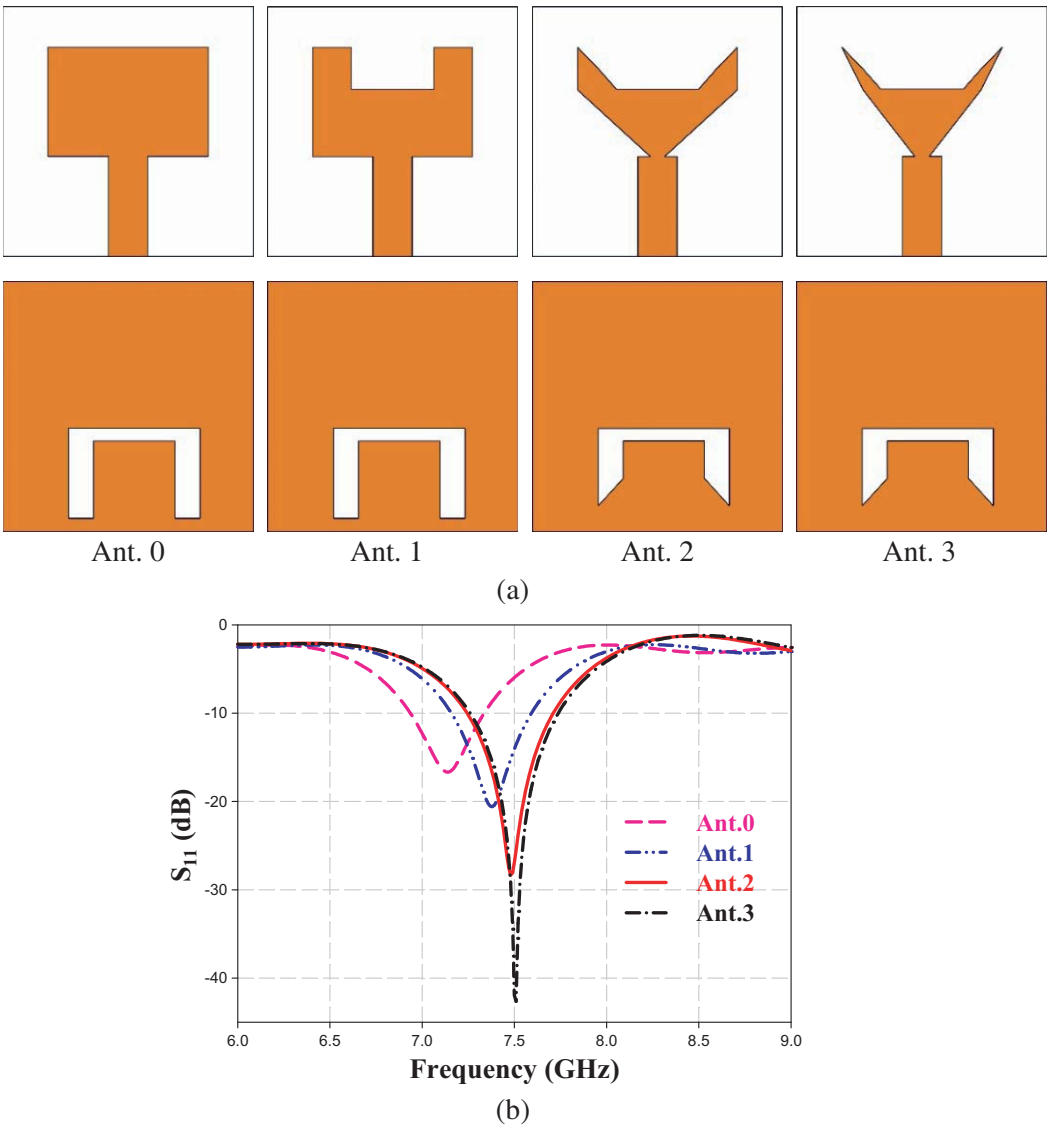

Figure 1. (a) Antenna design procedure. (b) Different step reflection coefficient.

2.2. Four-Element MIMO Antenna

The increase of the number of transmitter and receiver antennas can enhance the communication quality and increase the channel capacity without extra radiation power and spectrum bandwidth. In this section, four symmetrical monopole antenna elements printed on the top face of the substrate and four symmetrical U-slots etched on the bottom for X-band applications are presented with an overall size of $40 \times 40\,\text{mm}^2$. Each antenna element is fed by a $50\,\Omega$ microstrip line. As depicted in Figure 3, the compact design of a quad-element MIMO antenna is proposed, which are indicated by P1, P2, P3, and P4.

The simulated S-parameters of the proposed four-element MIMO antenna versus frequency is illustrated in Figure 4. Due to symmetry, the analysis of the S-parameter can be easily carried out by considering $S_{11} = S_{22} = S_{33} = S_{44}$, $S_{21} = S_{12} = S_{34} = S_{43}$, $S_{13} = S_{31} = S_{42} = S_{24}$, and $S_{14} = S_{41} = S_{23} = S_{32}$.

According to this figure, the reflection coefficient $|S_{11}|$ is adapted, with 42 dB at the desired frequency band (7.5 GHz). The impedance bandwidth of the proposed antenna is about 430 MHz (7.28 GHz–7.71 GHz). The isolation between port 1 and port 2/port 3, which are indicated by $|S_{12}|$ and

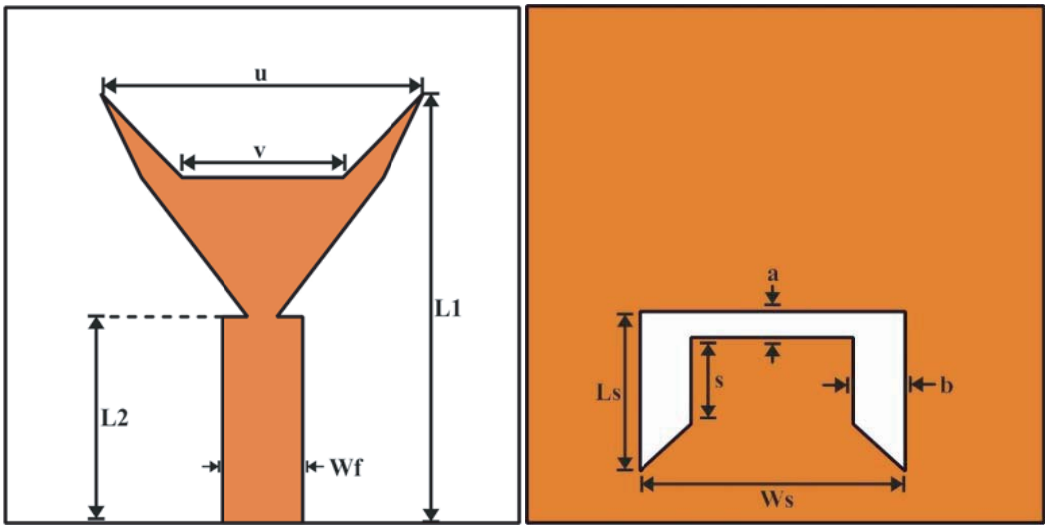

Figure 2. Geometry of the proposed single element antenna. (a) Top view. (b) Bottom view.

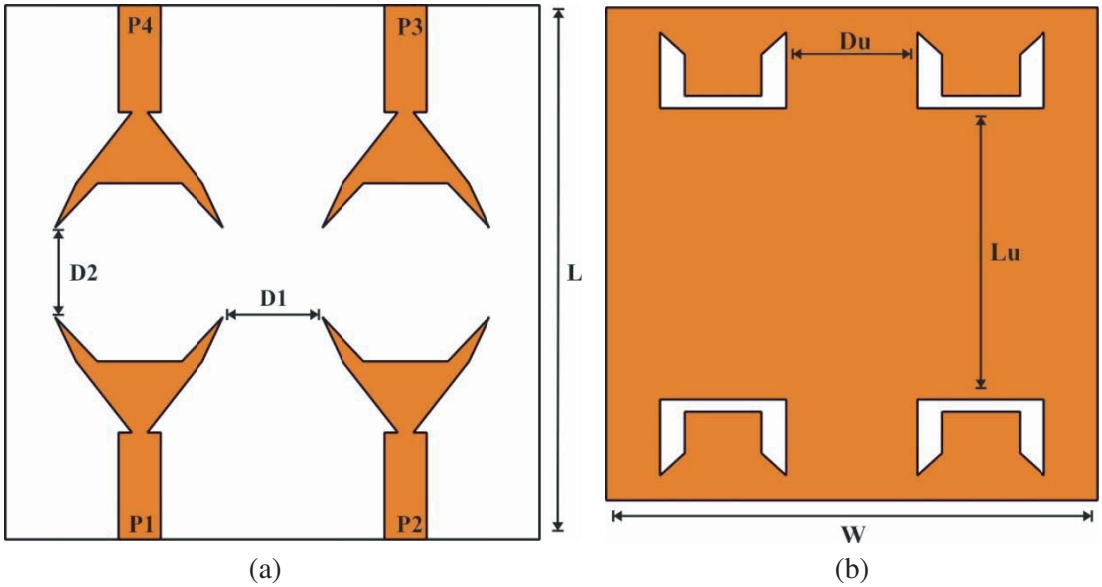

Figure 3. Design of the proposed four-element MIMO antenna. (a) Front view. (b) Bottom view.

$|S_{13}|$, is very high and more than 33 dB and 35 dB at the operating frequency band, respectively. The minimum isolation of the proposed antenna is nearly 26 dB at 7.5 GHz between port 1 and port 4 which proves the good performance of proposed quad-element MIMO antenna.

3. ANTENNA PERFORMANCE

3.1. Fabrication and Measurement

The proposed MIMO antenna has been fabricated and tested in order to validate the simulated results. The fabrication and measurement process is carried out at Abdel Malek Essaâdi University laboratories. It is done using a printed circuit board (PCB) milling machine: The LPKF Protomat E33.

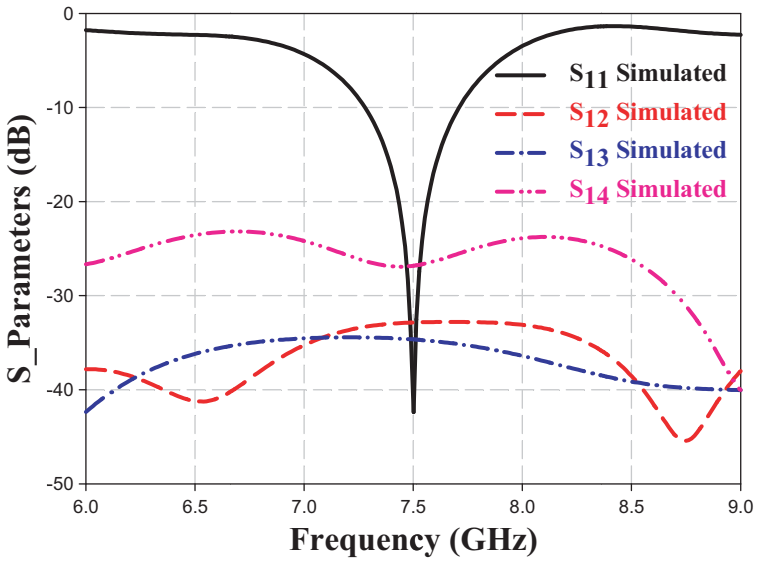

Figure 4. S-parameters result.

Figure 5 shows the top and bottom pictures of the fabricated four-element MIMO antenna. S-parameters of this antenna are measured by a Rohde and Schwarz ZVB 20 vector network analyzer. Since the four monopoles are symmetrically placed, only $|S_{11}|$, $|S_{12}|$, $|S_{13}|$, and $|S_{14}|$ curves are given. The measured -10 dB impedance bandwidth is 580 MHz (7.26 GHz–7.84 GHz) with 33 dB at the desired frequency band and covers a satellite communication system in the X-band (7.2–7.8 GHz).

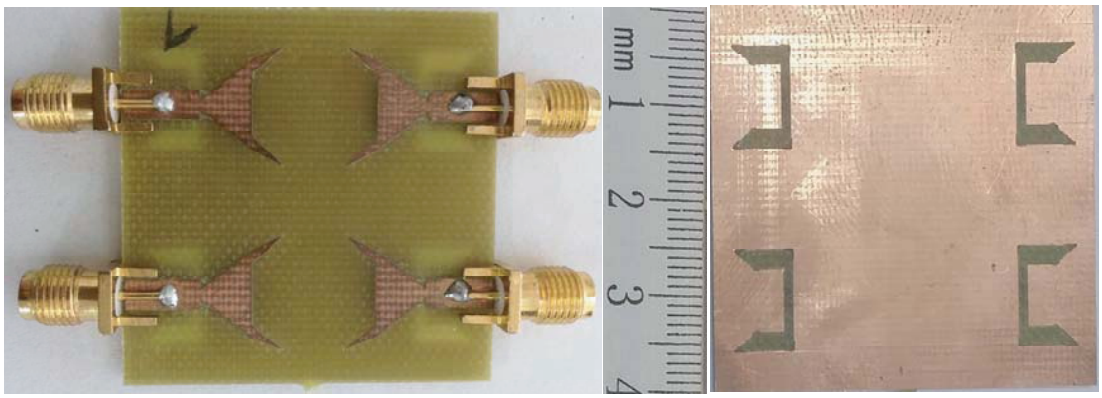

(a) (b)

Figure 5. Photograph of the fabricated MIMO antenna. (a) Top side. (b) Back side.

Also, the measured isolations of S_{12}, S_{13}, and S_{14} are higher than 24 dB at 7.5 GHz, which implies MIMO good performance.

Measured and simulated S parameters comparisons of the MIMO system are shown in Figure 6, which are in reasonable agreement. The small discrepancies between the responses are due to possible fabrication errors, parasitic effects, and SMA connectors losses.

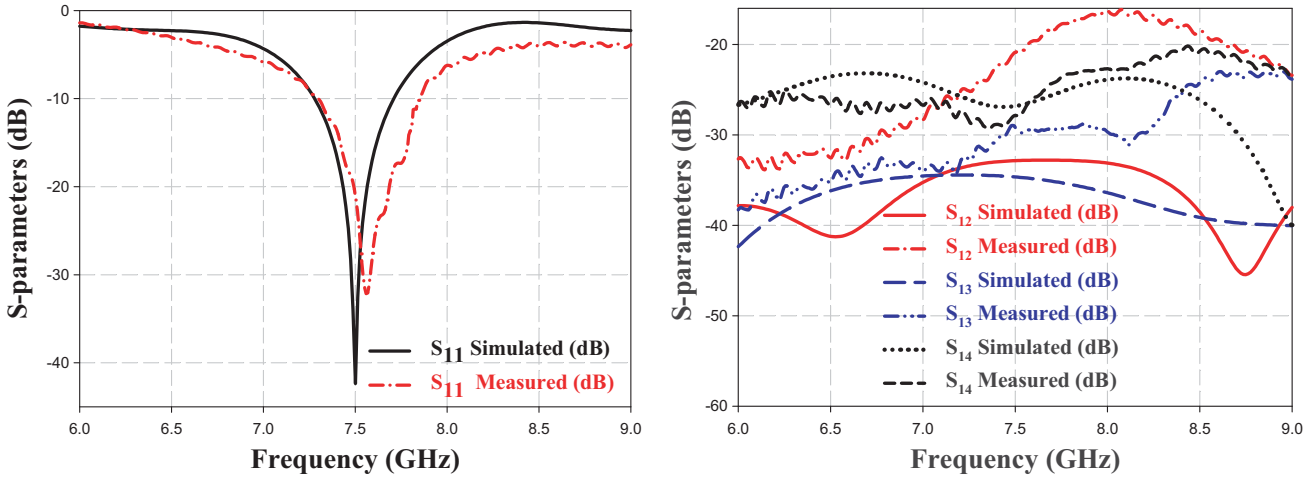

Figure 6. Measured and simulated S_{11}, S_{12}, S_{13} and S_{14} of the fabricated four elements MIMO antenna.

3.2. Envelope Correlation Coefficient and Diversity Gain

The envelope correlation (ECC) between the ith and jth antenna elements using far-field patterns [20] can be calculated from Eq. (1):

$$ECC\left(i,j\right)=\frac{\left(\oint\left(X_{PR}E_{\theta i}\left(\Omega\right)E_{\theta j}^{*}\left(\Omega\right)P_{\theta}\left(\Omega\right)+E_{\phi i}\left(\Omega\right)E_{\phi j}^{*}\left(\Omega\right)P_{\phi}\left(\Omega\right)\right)d\left(\Omega\right)\right)^{2}}{\oint\left(X_{PR}G_{\theta i}\left(\Omega\right)P_{\theta}\left(\Omega\right)+G_{\phi i}\left(\Omega\right)P_{\phi}\left(\Omega\right)\right)d\left(\Omega\right)\cdot\oint\left(X_{PR}G_{\theta j}\left(\Omega\right)P_{\theta}\left(\Omega\right)+G_{\phi j}\left(\Omega\right)P_{\phi}\left(\Omega\right)\right)d\left(\Omega\right)} \tag{1}$$

where X_{PR} denotes the cross-polarization power ratio of the propagation environment. In the formula above, $G_{\theta}(\Omega)=E_{\theta}(\Omega)E_{\theta}^{*}(\Omega)$ and $G_{\phi}(\Omega)=E_{\phi}(\Omega)E_{\phi}^{*}(\Omega)$ are the power patterns of θ and ϕ polarizations, respectively. $P_{\theta}(\Omega)$ and $P_{\phi}(\Omega)$ denote the angular density functions of θ and ϕ polarizations, respectively.

$E_{\theta i}(\Omega)$ and $E_{\theta j}(\Omega)$ are the electric field patterns of the ith and jth antenna elements in the θ polarization, respectively. $E_{\phi i}(\Omega)$ and $E_{\phi j}(\Omega)$ are the electric field patterns of the ith and jth antenna elements in the ϕ polarization, respectively.

In the uniform multipath environment case, $X_{PR}=1$ and $P_{\theta}(\Omega)=P_{\phi}(\Omega)=\frac{1}{4\pi}$.

The envelope correlation coefficient ECC for two antennas can be approximated as follows:

$$ECC=\frac{\left(\oint\left(E_{\theta1}\left(\Omega\right)E_{\theta2}^{*}\left(\Omega\right)+E_{\phi1}\left(\Omega\right)E_{\phi2}^{*}\left(\Omega\right)\right)d\left(\Omega\right)\right)^{2}}{\oint\left(G_{\theta1}\left(\Omega\right)+G_{\phi1}\left(\Omega\right)\right)d\left(\Omega\right)\cdot\oint\left(G_{\theta2}\left(\Omega\right)+G_{\phi2}\left(\Omega\right)\right)d\left(\Omega\right)} \tag{2}$$

In the case of a (4, 4) MIMO system, with $N=4$ antennas at both ends, the envelope correlations between antennas $i=1$ and $j=2,3,4$ are shown in Figure 7, where $ECC(1,2)$, $ECC(1,3)$, and $ECC(1,4)$ are envelope correlations between antennas 1 & 2, antennas 1 & 3, and antennas 1 & 4, respectively. The envelope correlation in the interested frequency band is less than 0.02 which is good enough for MIMO applications.

The diversity gain can be given by the following approximate expression [21, 22].

$$DG=10\sqrt{\left(1-\left|\rho\right|^{2}\right)} \tag{3}$$

where ρ is the complex cross correlation coefficient, and $|\rho|^{2}=ECC$.

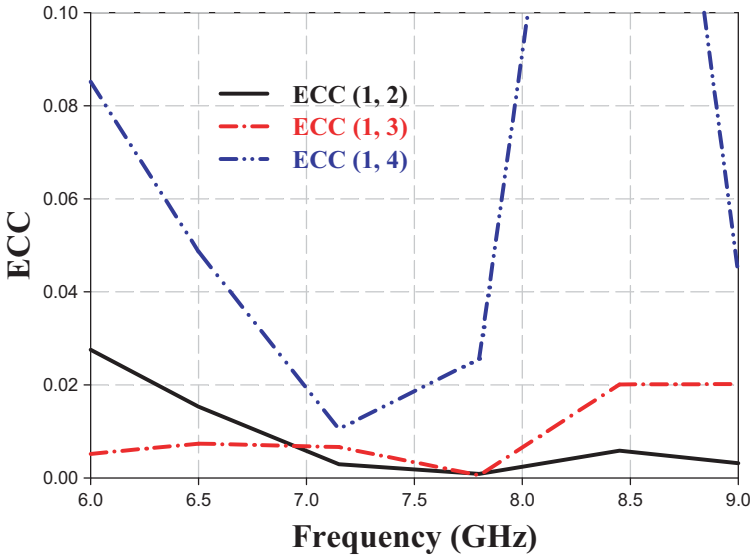

Figure 7. The ECC curve.

Figure 8 illustrates the simulated diversity gain of the MIMO system. From these curves, we can see clearly that the diversity gain from far-field patterns is around 9.95 dB at the operating frequency (7.5 GHz).

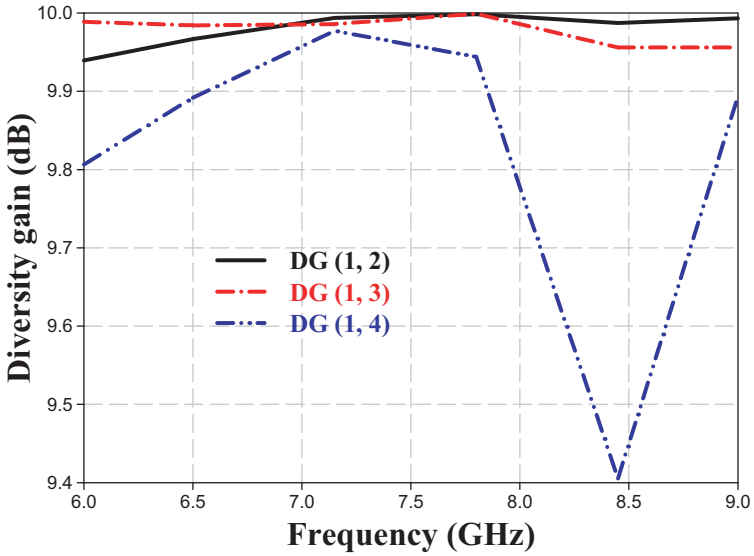

Figure 8. The DG curve.

3.3. Radiation Patterns

The comparisons results between measured and simulated radiation patterns in terms of E-plane (xoy-plane) and H-plane (yoz-plane) at 7.5 GHz are shown in Figure 9. It shows that the E-plane radiation pattern is of the shape of nearly symbol of '8' at 7.5 GHz, but the H-plane radiation pattern is purely omnidirectional (form of 'O') at 7.5 GHz. The measurements of radiation patterns are not carried out in an anechoic chamber but in a free space, and for that the measured result is slightly distorted compared with the simulated one.

Table 2. Comparisons among this work and recent published four elements MIMO antennas.

Reference		SIZE (mm^3)	Bandwidth (%)	Minimum isolation	ECC	Sub.
2×2 MIMO ANTENNA	[23]	$70 \times 50 \times 0.4$ $1.71\lambda_g \times 1.22\lambda_g \times 0.01\lambda_g$	14.49/9.43/11.26	> 19.63	0.0014	FR-4
	[24]	$50.54 \times 21.29 \times 1.6$ $2.00\lambda_g \times 0.84\lambda_g \times 0.06\lambda_g$	5.43/5.27	> 18.43	0.2	FR-4
	[25]	$42 \times 17 \times 1.6$ $2.11\lambda_g \times 0.85\lambda_g \times 0.08\lambda_g$	25.45	> 13	0.015	FR-4
4×4 MIMO ANTENNA	[26]	$40 \times 40 \times 1.6$ $0.75\lambda_g \times 0.75\lambda_g \times 0.03\lambda_g$	58.6	> 11	< 0.1	FR-4
	[27]	$73 \times 54.7 \times 1.6$ $2.68\lambda_g \times 2.01\lambda_g \times 0.058\lambda_g$	4.73	> 35	-	FR-4
	This work	$40 \times 40 \times 1.6$ $0.47\lambda_g \times 0.47\lambda_g \times 0.08\lambda_g$	7.68	> 26	< 0.02	FR-4

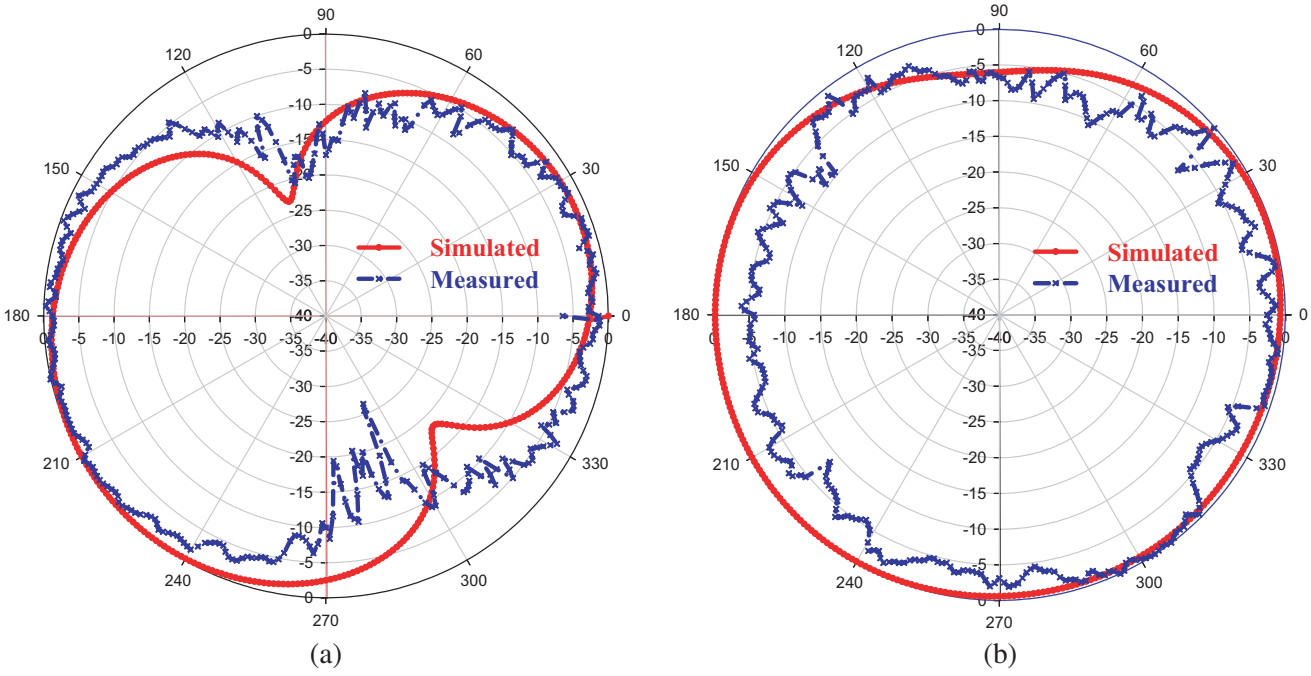

(a) (b)

Figure 9. The measured and simulated radiation patterns of the proposed MIMO antenna: (a) *E*-plane, (b) *H*-plane.

As can be seen in Table 2, the proposed structure has a compact size, low ECC, and high isolation at the operating frequency band as compared to published four elements MIMO antennas.

4. CONCLUSION

In this paper, a compact planar quad-element mono-band MIMO antenna with low mutual coupling for X-band applications is presented. The proposed structure, operating at 7.5 GHz, has a simple structure with a compact size of $40 \times 40\,\text{mm}^2$. Measured results show that the proposed antenna has an impedance bandwidth of 580 MHz (7.26 GHz–7.84 GHz) with high isolation (more than 24 dB) at the operating frequency band. Furthermore, the proposed structure has a good diversity performance at the resonance frequency band, with high diversity gain and low ECC values of 9.95 dB and 0.02, respectively.

REFERENCES

1. Soltani, S. and R. D. Murch, "A compact planar printed MIMO antenna design," *IEEE Trans. Antennas Propag.*, Vol. 63, 1140–1149, 2015.
2. Ahmed, B. T., P. S. Olivares, J. L. M. Campos, and F. M. Vázquez, "3.1–20 GHz MIMO antennas," *AEU — International Journal of Electronics and Communications*, Vol. 94, 348–358, 2018.
3. Lo, T. K. and Y. Hwang, "Microstrip antennas of very high permittivity for personal communications," *1997 Asia Pacific Microwave Conference*, 253–256, 1997.
4. Yang, B., M. Chen, and L. Li, "Design of a four-element WLAN/LTE/UWB MIMO antenna using half-slot structure," *International Journal of Electronics and Communications*, Vol. 93, 354–359, 2018.
5. Acharjee, J., K. Mandal, and S. K. Mandal, "Reduction of mutual coupling and cross-polarization of a MIMO/diversity antenna using a String of H-shaped DGS," *AEU — International Journal of Electronics and Communications*, Vol. 97, 110–119, 2018.
6. Manouare, A. Z., S. Ibnyaich, A. El Idrissi, and A. Ghammaz, "Miniaturized triple wideband CPW-fed patch antenna with a defected ground structure for WLAN/WiMAX applications," *Journal of Microwaves, Ptoelectronics and Electromagnetic Applications*, Vol. 15, No. 3, 157–169, Sep. 2016.
7. Banerjee, J., A. Karmakar, R. Ghatak, and D. R. Poddar, "Compact CPW-fed UWB MIMO antenna with a novel modified Minkowski fractal Defected Ground Structure (DGS) for high isolation and triple bandnotch characteristic," *Journal of Electromagnetic Waves and Applications*, Vol. 31, No. 15, 1550–1565, 2017.
8. Kamal, S. and A. A. Chaudhari, "Printed meander line MIMO antenna integrated with air gap, DGS and RIS: A low mutual coupling design for LTE applications," *Progress In Electromagnetics Research C*, Vol. 71, 149–159, 2017.
9. Bhadouria, A. S. and M. Kumar, "Microstrip X-band antenna with improvement in performance using DGS," *Electrical and Electronic Engineering*, Vol. 4, No. 2, 31–35, 2014.
10. Kumar, N. and U. K. Kommuri, "MIMO antenna mutual coupling reduction for WLAN using spiro meander line UC-EBG," *Progress In Electromagnetics Research C*, Vol. 80, 65–77, 2018.
11. Dabas, T., D. Gangwar, B. K. Kanaujia, and A. K. Gautam, "Mutual coupling reduction between elements of UWB MIMO antenna using small size uniplanar EBG exhibiting multiple stop bands," *AEU — International Journal of Electronics and Communications*, Vol. 93, 32–38, 2018.
12. Wu, W., B. Yuan, and A. Wu, "A quad-element UWB-MIMO antenna with band-notch and reduced mutual coupling based on EBG structures," *International Journal of Antennas and Propagation*, Vol. 2018, 10 pages, 2018.
13. Lee, Y., H. Chung, J. Ha, and J. Choi, "Design of a MIMO antenna with improved isolation using meta-material," *International Journal of Antennas and Propagation*, 231–234, Mar. 2011.
14. Chen, X., B. Feng, Q. Zeng, and K. L. Chung, "A substrate integrated magneto-electric dipole antenna and its 3D MIMO system with metasurface for 5G/WiMAX/WLAN/X-BAND applications," *2017 International Symposium on Antennas and Propagation (ISAP)*, Phuket, Thailand, Oct. 30–Nov. 2, 2017.

15. Nirdosh, C. M. Tan, and M. R. Tripathy, "A miniaturized T-shaped MIMO antenna for X-band and Ku-band applications with enhanced radiation efficiency", *2018 27th Wireless and Optical Communication Conference (WOCC)*, Hualien, Taiwan, Apr. 30–May 1, 2018.
16. Nirdosh, A. Kakkar, and S. Sah, "A two-element wideband MIMO antenna for X band, Ku-band, K-band applications," *2018 5th International Conference on Signal Processing and Integrated Networks (SPIN)*, Noida, India, Feb. 22–23, 2018.
17. Sun, D. and C. Wei, "Analysis and design of 4×4 MIMO-antenna systems in mobile phone," *Journal of Computer and Communications*, 26–33, 2016.
18. Kumari, T., G. Das, A. Sharma, and R. Kumar, "Design approach for dual element hybrid MIMO antenna arrangement for wideband applications," *Int. J. RF Microwave Computer Aided Eng.*, 1–10, 2018.
19. Wang, Z., L. Zhao, Y. Cai, S. Zheng, and Y. Yin, "A Meta-surface Antenna Array Decoupling (MAAD) method for mutual coupling reduction in a MIMO antenna system," *Scientific Reports*, 1–9, 2018.
20. Zhang, J., J. Ou Yang, K. Z. Zhang, and F. Yang, "A novel dual-band MIMO antenna with lower correlation coefficient," *International Journal of Antennas and Propagation*, Vol. 2012, Article ID 512975, 7 pages, 2012.
21. Pierce, J. N. and S. Stein, "Multiple diversity with non independent fading," *Proceedings of the IRE*, Vol. 48, 89–104, Jan. 1960.
22. Schwartz, M., W. R. Bennett, and S. Stein, *Communication System and Techniques*, 470–474, McGraw-Hill, New York, 1965.
23. Vasu Babu, K. and B. Anuradha, "Tri-band MIMO antenna for WLAN, WiMAX and defence system & radio astronomy applications," *Advanced Electromagnetics*, Vol. 7, No. 2, Mar. 2018.
24. Satam, V. and S. Nema, "Defected ground structure planar dual element MIMO antenna for wireless and short range RADAR application," *2015 IEEE International Conference on Signal Processing, Informatics, Communication and Energy Systems (SPICES)*, Kozhikode, India, Feb. 19–21, 2015.
25. Pouyanfar, N., C. Ghobadi, J. Nourinia, K. Pedram, and M. Majidzadeh, "A compact multi-band MIMO antenna with high isolation for C and X bands using defected ground structure," *Radioengineering*, Vol. 27, No. 3, 686–693, 2018.
26. Sarkar, D. and K. V. Srivastava, "A compact four-element MIMO/diversity antenna with enhanced bandwidth," *IEEE Antennas and Wireless Propagation Letters*, Vol. 16, 2469–2472, 2017.
27. Ghosh, C. K., "A compact 4-channel microstrip MIMO antenna with reduced mutual coupling," *AEU — International Journal of Electronics and Communications*, Vol. 70, No. 7, 873–879, Jul. 2016.